UCRL 3911/80

UNIVERSITY OF CALIFORNIA

Ernest O. Lawrence Radiation Laboratory

TWO-WEEK LOAN COPY

This is a Library Circulating Copy which may be borrowed for two weeks. For a personal retention copy, call Tech. Info. Division, Ext. 5545

BERKELEY, CALIFORNIA

DISCLAIMER

This document was prepared as an account of work sponsored by the United States Government. While this document is believed to contain correct information, neither the United States Government nor any agency thereof, nor the Regents of the University of California, nor any of their employees, makes any warranty, express or implied, or assumes any legal responsibility for the accuracy, completeness, or usefulness of any information, apparatus, product, or process disclosed, or represents that its use would not infringe privately owned rights. Reference herein to any specific commercial product, process, or service by its trade name, trademark, manufacturer, or otherwise, does not necessarily constitute or imply its endorsement, recommendation, or favoring by the United States Government or any agency thereof, or the Regents of the University of California. The views and opinions of authors expressed herein do not necessarily state or reflect those of the United States Government or any agency thereof or the Regents of the University of California.

UCRL-3911 Rev.

UNIVERSITY OF CALIFORNIA

Lawrence Radiation Laboratory
Berkeley, California

Contract No. W-7405-eng-48

LONGITUDINAL DISPERSION IN TWO-PHASE CONTINUOUS-FLOW OPERATIONS: CALCULATION METHODS

Terukatsu Miyauchi, Alice K. McMullen, and Theodore Vermeulen

March 1960

Printed for the U. S. Atomic Energy Commission

LONGITUDINAL DISPERSION IN TWO-PHASE CONTINUOUS-FLOW OPERATIONS: CALCULATION METHODS

Terukatsu Miyauchi, Alice K. McMullen, and Theodore Vermeulen

Lawrence Radiation Laboratory and Department of Chemical Engineering
University of California, Berkeley, California

March 1960

ABSTRACT

The effect of longitudinal dispersion upon concentration or temperature profiles is shown graphically, for individual complete profiles, for outlet concentrations under a range of conditions, and for the ratio of the concentration change at the inlet to the over-all concentration change. In addition, an algebraic correlation is given for "exterior apparent" NTU, as a function of "true" NTU and of a suitably defined "number of over-all dispersion units." These calculational tools are intended to facilitate the analysis of longitudinal-mixing effects in operating equipment.

LONGITUDINAL DISPERSION IN TWO-PHASE CONTINUOUS-FLOW OPERATIONS: CALCULATION METHODS*

Terukatsu Miyauchi, Alice K. McMullen, and Theodore Vermeulen

Lawrence Radiation Laboratory and Department of Chemical Engineering
University of California, Berkeley, California

March 1960

Exact mathematical relations are available, for example in the foregoing paper (3), for calculating the concentration or temperature profiles in non-staged contacting equipment (e.g. absorption or extraction columns, or tubular heat exchangers) under such conditions that the pertinent physical parameters are constant throughout the length of the column. These parameters are the longitudinal-dispersion coefficient for each phase, the over-all "true" coefficient of mass or heat transfer, and the capacity ratio (or product of flowrate ratio and solute partition coefficient).

Tables have recently been computed for many representative combinations of these variables (4,5). This study provides typical graphs of the tabulated functions, in a form which allows more direct application for interpreting experimental data. It also gives an approximate interpolation method for relating the "number of over-all dispersion units," the number of over-all mass- (or heat-) transfer units, and the actual performance of equipment, so as to permit calculation of any one of these properties if the other two are known. Although countercurrent flow is emphasized, a few results are also shown for cocurrent flow.

---

*This work was performed under the auspices of the U. S. Atomic Energy Commission.

NUMERICAL RESULTS FOR CONCENTRATION PROFILES

The diffusion-equation model for longitudinal dispersion, used in preceding papers, yields the relative outlet concentration or temperature values (6), and also the profile of values for each phase throughout the length (3). Various sets of values of the parameters correspond to the same "exterior" performance, or combination of inlet and outlet concentrations; but each set of parameter values corresponds uniquely to a particular pair of "interior" profiles. Experimental knowledge of the complete profiles is therefore an essential factor in proving that the theory does apply adequately to given types of flow equipment, and in confirming the numerical rates of dispersion and of interphase transport that are assigned.

The following dimensional variables are used:

(a) For each phase: superficial velocity F_i; superficial axial dispersion coefficient E_i, analogous to a diffusivity; mixing length $\ell_i = E_i/F_i$; concentration c_i or temperature t_i.

(b) For the two phases together: over-all transfer coefficient k_{oi}, or height of over-all transfer unit $H_{oi} = F_i/k_{oi}a$, expressed relative to either phase; partition coefficient $m = dc_x^*/dc_y$ (which is unity in heat transfer); length within the column, z, measured from the X-phase inlet; characteristic length d (for instance, the particle diameter d_p in packed beds>; total column length L.

From these, nine dimensionless variables are developed:

1,2, Column Péclet numbers, P_xB and P_yB, with $B = d/L$ and $P_i = \ell_i/d$.

3, Capacity ratio, or extraction factor, $A = mF_x/F_y$.

4, Number of true over-all transfer units (relative to the X phase), $N_{ox} = L/H_{ox} = k_{ox}aL/F_x$.

5 Fractional length, $Z = z/L$.

6,7, Dimensionless "concentrations," $C_i = c_i/c_{x0}$ or t_i/t_{x0}, where subscript 0 denotes the inlet value.

8,9, Generalized concentrations X and Y, with

$$X = \frac{C_x - (Q + mC_y^{\,1})}{1 - (Q + mC_y^{\,1})} \tag{1}$$

and

$$Y = \frac{m(C_y - C_y^{\,1})}{1 - (Q + mC_y^{\,1})} \tag{2}$$

Solutions of the diffusion-type differential equations, using these dimensionless variables, are obtained in the form

$$X = X(N_{ox}, A, P_xB, P_yB, Z),$$

$$Y = Y(N_{ox}, A, P_xB, P_yB, Z).$$

The behavior of these solutions is examined in some detail.

Countercurrent Case

The general solution for this case, reported in the preceding paper, has been evaluated numerically on an IBM 701 computer. Figure 1, in block-diagram form, shows the computation program that was used. Values of X and Y have been tabulated to the fourth decimal place (4) for the following range of variables:

$A = \frac{1}{16}, \frac{1}{8}, \frac{1}{4}, \frac{1}{2}, 1, 2, 4, 8, 16,$

$N_{ox} = 1, 2, 4, 8;$ in some cases also 16, 32, 64,

$P_xB = \frac{1}{4} N_{ox}, N_{ox}, 4 N_{ox},$

$P_yB = \frac{1}{8} P_xB, \frac{1}{2} P_xB, P_xB, 2 P_xB, 8 P_xB,$

$Z = 0, 0.05, 0.15, 0.50, 0.85, 0.95, 1.00.$

The fractional-length (Z) values were selected to permit construction of the entire profile by graphical interpolation. The curvature of any profile increases toward the outlet end, since at this point a zero slope is reached. Plots of typical profiles (with $P_xB = P_yB$ in each) are given for the following cases:

$\Lambda = 1$: $N_{ox} = 1$ and 4 (Figure 2). The uniformly varying piston-flow case is shown by the $P_xB = \infty$ lines. Perfect mixing in both phases ($P_xB = P_yB = 0$), not shown, corresponds to a horizontal line at $X = (\Lambda N_{ox} + 1)/(\Lambda N_{ox} + N_{ox} + 1)$; i.e., 0.667 and 0.555, respectively. Because of the inversion relations discussed below, Figure 2 is also a plot of Y against Z but with the coordinates reversed.

$\Lambda = \frac{1}{4}$: $N_{ox} = 1$ and 4 (Figure 3). Again the range from no mixing to almost complete mixing is given; now the horizontal-line limits are $X = 0.555$ and $X = 0.333$. With the capacity ratio inverted, this becomes a plot of Y versus Z at a new pair of N_{ox} values.

$\Lambda = 4$: $N_{ox} = 1$ and 4 (Figure 4). The horizontal-line limits for X are 0.833 and 0.810. The curves for $N_{ox} = 1$, here, are the complements of those for $N_{ox} = 4$ in Figure 3; that is, if one figure describes the X-phase behavior in a column, the other describes the accompanying Y-phase behavior.

Inversion relations exist because of symmetry in designating the X and Y phases. If actual changes in generalized concentration were calculated and were compared with the total possible change to give a "percentage of completion," the X and Y phases would lose their identification with raffinate and extract, or with warm and cool fluid, and would become completely arbitrary. As discussed in the preceding paper, the inverted functions (designated with the dagger†) are given by

$$\Lambda^{\dagger} = (\Lambda)^{-1} \; ; \quad N_{ox}{}^{\dagger} = \Lambda N_{ox} \; ; \; P_x{}^{\dagger}B = P_yB,$$

$$Y^{\dagger} = 1 - X \; ; \quad X^{\dagger} = 1 - Y. \tag{3}$$

For countercurrent flow, also, $Z^{\dagger} = 1 - Z$.

The separate effects of P_xB and P_yB can be shown graphically if the other variables are reduced in number; for instance, by setting $Z = 1$, and plotting only the outlet concentration X_1. Figure 5 shows the variation in X_1 that can occur at a specific pair of parameter values: $\Lambda = 1$, $N_{ox} = 4$. The abscissa is P_xB, on a nonlinear scale, while the contours correspond to different P_yB values. Perfect mixing in one phase, with complete absence of mixing in the other, is represented by the uppermost right-hand point and the lowermost left-hand point; if Λ were not equal to unity, the corresponding X_1 values would not be equal.

Cocurrent Case

Tables similar to the above have been calculated for parallel flow of the phases in contact (5), corresponding to the solution given for this case in the preceding paper. In this case, the inversion relation for fractional length is $Z^{\dagger} = Z$, while the other variables still conform to Equation 3. Because $Y^{\dagger}$ is now related to X at the same Z, conversion of X to $Y^{\dagger}$ is facilitated; and the tabulated range of variables has therefore been reduced (compared with those covered for countercurrent flow) by eliminating Λ values greater than 2.

Typical profiles are given in Figure 6, for $\Lambda = \frac{1}{4}$ and $\Lambda = 4$. It appears that cocurrent flow will always give plots that are concave upward on X-Z coordinates, unlike the countercurrent profiles with $\Lambda > 1$ typified by Figure 4.

Outlet Concentration for One Phase, with Negligible Concentration Change Occurring in the Other

If one of two phases (say, the Y phase) is supplied at large flowrates (i.e., $F_y \to \infty$), or provides an irreversible outlet for the solute ($m \to 0$), the capacity ratio becomes vanishingly small ($\Lambda \to 0$). Under these conditions, the Y phase has, either actually or effectively, an entirely uniform concentration from entrance to exit. Within the apparatus, regardless of the flow pattern, the Y phase acts as if it underwent perfect mixing ($P_yB = 0$). Therefore it is convenient to use the equations for perfect mixing in one phase (Case 5 in Table I of the preceding paper) as a starting point for introducing the condition that $\Lambda = 0$.

The X-phase concentration will continue to show the inlet discontinuity and subsequent continual decrease characteristic of longitudinal dispersion. It is possible to describe its behavior by a still simpler equation than for $P_yB = 0$. If the condition that $\Lambda = 0$ is added, then in the Case 5 equation $E = 0$ and $X = F/D$. The equation for outlet concentration, with some rearrangement, then becomes

$$(X_1)_{\Lambda \to 0} = \frac{4\nu e^{P_xB/2}}{(1+\nu)^2 e^{P_xB/2} - (1-\nu)^2 e^{-P_xB/2}}, \tag{4}$$

with $\nu = (1 + 4N_{ox}/P_xB)^{1/2}$. A similar result has been obtained for first-order chemical reaction in single-phase flow (2,8).

Exterior-apparent NTU, N_{oxP}, is related to outlet concentration by the Colburn equation (1), as discussed in the preceding paper. In the case discussed here this becomes

$$(X_1)_{\Lambda \to 0} = e^{-N_{oxP}} \tag{5}$$

or

$$N_{oxP} = -\ln(X_1)_{\Lambda \to 0} . \tag{5a}$$

Thus, for $\Lambda = 0$, either X_1 or N_{oxP} can be calculated from N_{ox} and P_xB by use of Equations 4 and 5. The resulting numerical relations are plotted in Figure 7. Concentrations other than the outlet values are not given by Figure 7, but can be calculated from the relation $X = F/D$.

INLET DISCONTINUITY AS A MEASURE OF PERFORMANCE

If the complete concentration profiles in a column are not specified, a good indication of its behavior can still be had by knowing the interior concentrations at the inlet ends (X_0, Y_1), together with the outlet values ($X_1 = X^1$, $Y_0 = Y^0$). In any experiment, the mathematical discontinuity at the inlet is not achieved completely, because the dispersion coefficient is likely not to remain constant at the ends of the equipment. Hence it is best to estimate X_0 and Y_1 by extrapolation from the X and Y values at other interior points.

Each discontinuity depends primarily upon the three variables Λ, N_{ox}, and PB for the phase involved, and secondarily upon PB for the other phase. As a result, any one set of the four independent variables corresponds uniquely to some one set of four terminal interior concentrations X_0, X_1, Y_1, Y_0.

With previous knowledge only of Λ, and not of either dispersivities or transfer coefficients, it is necessary to apply trial-and-error procedures in order to find the values of the controlling variables that match the experimental concentration data.

Plots of X_0 or Y_1

Direct plotting of X_0 or Y_1 is one evident method. Figure 8 shows X_0 as a function of N_{ox} and P_xB, with P_yB and Λ specified (both zero); here X_0 is

determined from the equation $X = F/D$, which corresponds as above to Case 5 in the preceding paper. Similar diagrams for other cases can be calculated from the respective equations, or from the numerical tables available (4,5).

"Jump Ratio" Plots

Better groundwork could be laid for trial-and-error procedures if the multiplicity of graphs like Figure 8 could be reduced. This would require finding a variable to which concentration is relatively insensitive, such as P_1B for the opposite phase, as already cited. Further simplification can be brought about by using a secondary function of experimental concentration values, the jump ratio, defined as follows for the two phases:

$$r_x = (1 - X_0)/(1 - X_1),$$
$$r_y = Y_1/Y_0 . \qquad (6)$$

For either phase, then, r is the difference between the feed concentration and the inlet-end interior concentration, divided by the difference between feed and outlet concentrations. This ratio is much less sensitive to N_{ox} than the X_0 or Y_1 values themselves.

Figure 9 shows a particularly favorable case for using the r_x and r_y values, at $\Lambda = 1$. The plotted values have been obtained from the available concentration-profile tables (4). A complete grid of contours is given here for $N_{ox} = 2$; and a partial grid, with every second value of P_1B, for $N_{ox} = 8$. If N_{ox} is known only to within 50%, the P_1B values can be determined to within about 10%. The resulting estimates can be used with the X_1 value, by methods to be described below, to provide a better estimate of N_{ox}. This in turn gives better values of the P_1B's, and the process can be repeated as many times as necessary.

A similar plot for $\Lambda = 4$ is given in Figure 10. Here an accurately known pair of r values, taken with a 50% error in N_{ox}, can give a 25% error in P_xB or P_yB. Figure 11 shows the relationships for $\Lambda = 16$, and gives about the same error in P_iB's as is introduced in N_{ox}. Even this large discrepancy does not prevent convergence after iteration through several cycles.

The inversion relations are utilized in Figures 10 and 11, to make them applicable also to case of $\Lambda = 1/4$ and 1/16. For such use, it should be remembered that $P_x^{\dagger}B = P_yB$, and $P_y^{\dagger}B = P_xB$. Plots at intermediate values of Λ -- i.e., 2 and 1/2, and 8 and 1/8 -- could also be prepared from the tables available. For a Λ applicable to any particular experiment, interpolation between the graphs already available would probably be preferable to re-solving the exact equation by machine computation to develop an entire new table.

The present tables do not cover Λ values outside the range of 1/16 to 16. For such extreme values, it would be desirable to test the applicability of $\Lambda = 0$ behavior, with inversion of the designations of the two phases if necessary.

Another type of limiting behavior is shown in Figure 12, applicable where column performance is determined entirely by dispersion phenomena -- i.e., for $N_{ox} \to \infty$. For this situation, the mixing effects in the two phases can not be identified separately; they are combined algebraically in what amounts to a separate function, defined as $P_{oy}B$ in the preceding paper:

$$P_{oy}B = \left[\frac{\Lambda}{P_xB}\right] + \left[\frac{1}{P_yB}\right]^{-1} . \qquad (7)$$

A three-way confirmation that the infinite N_{ox} approximation is satisfactory, in a given case, is obtained if the $P_{oy}B$ values deduced from r_x, from r_y, and from X_1 are all equal. It is noted that Figure 12 applies to the full range of Λ values.

RAPID CALCULATION METHOD FOR EXTENT OF COMPLETION

The calculation of some one point on the concentration profile, such as X_0 or X_1, is inherently more simple than a computation of the entire profile. In this paper, it has been possible to describe X_0 by a series of graphs relating it to X_1. Elsewhere, Sleicher has given graphs illustrating the behavior of X_1 (6). An algebraic calculation method of X_1 will now be given which is less exact, but much faster, than the complete analytical solution represented by Figure 1.

The relation selected for this purpose takes its form from Miyauchi's equation for $N_{ox} \to \infty$ (Case 9 of the preceding paper). With $\Lambda \neq 1$, the generalized outlet concentration is

$$(X_1)_{N_{ox} = \infty} = \frac{(1 - \Lambda)\, \Lambda \exp \left[\dfrac{(\Lambda - 1)\, P_x B\, P_y B}{P_x B + \Lambda\, P_y B} \right]}{1 - \Lambda^2 \exp \left[\dfrac{(\Lambda - 1)\, P_x B\, P_y B}{P_x B + \Lambda\, P_y B} \right]} \quad . \tag{8}$$

This expression can be compared with the Colburn equation (1), used here to define the exterior apparent (or piston-flow-model) NTU:

$$X_1 = \frac{(1 - \Lambda) \exp \left[(\Lambda - 1)\, N_{oxP} \right]}{1 - \Lambda \exp \left[(\Lambda - 1)\, N_{oxP} \right]} \quad . \tag{9}$$

Combination of Equations 8 and 9, for the case in which $N_{ox} = \infty$ only, yields

$$(N_{oxP})_{N_{ox} = \infty} = \frac{\ell n\, \Lambda}{\Lambda - 1} + \left[\frac{\Lambda}{P_x B} + \frac{1}{P_y B} \right]^{-1} \quad . \tag{10}$$

(This relation is continuous through the value of $\Lambda = 1$; there $\ln \Lambda/(\Lambda - 1)$ is unity, and also $X = 1/(1 + N_{oxP})$.)

Since N_{oxP} is a function of N_{ox}, Λ, P_xB, and P_yB, it can be broken up arbitrarily into parts that retain this functional dependence. The behavior of N_{oxP} in the two limiting cases of mass transfer controlling and of longitudinal dispersion controlling is consistent with the addition of reciprocals,

$$\frac{1}{N_{oxP}} = \frac{1}{N_{ox}} + \frac{1}{N_{oxD}}, \qquad (11)$$

where N_{oxD} is the "number of over-all dispersion units," referred to the X phase -- evidently a function of Λ, P_xB, P_yB, and probably also of N_{ox}.

Equation 11 retains its validity if every term is multiplied by the column height h. The quotient $H_{ox} = h/N_{ox}$ is recognized as the customary true HTU. $H_{oxP} = h/N_{oxP}$ becomes the exterior apparent HTU; and $H_{oxD} = h/N_{oxD}$ becomes the "height of a dispersion unit." Thus, $H_{oxP} = H_{ox} + H_{oxD}$. This concept has been utilized in fixed-bed separation operations by Van Deemter et al. (7).

Combination of Equations 10 and 11 indicates that the former gives the limiting value of N_{oxD}, as $N_{ox} \to \infty$. This relation is therefore assumed to provide a general form for the evaluation of N_{oxD}:

$$N_{oxD} = \frac{\ln \Lambda}{\Lambda - 1}\,\phi + (PB)_y. \qquad (12)$$

As a first step toward possible correlation, Equation 12 was used with $\phi = 1$ and with $(PB)_y = P_{oy}B$ as calculated by Equation 7. Figure 13 shows the resulting correlation, in dashed curves, compared with the computer values as solid curves. Since the agreement seems adequate at $\Lambda = 1$ but not elsewhere,

it was concluded that the correlation had been put in suitable algebraic form but that a different definition of the over-all Péclet group would be necessary.

For this reason, $(PB)_y$ has been defined by the equation

$$(PB)_y = \left[\frac{\Lambda}{f_x P_x B} + \frac{1}{f_y P_y B}\right]^{-1} . \tag{13}$$

Here the weighting factors f_x and f_y are functions of N_{ox} and Λ; and ϕ may be a function of $(PB)_y$, N_{ox}, and Λ. In practice, ϕ is assumed to deviate from unity only in the region of low Péclet numbers where, because perfect mixing is approached, the mass-transfer framework of calculation is put to its severest test. The factors f_x and f_y are not true constants, but only average values which provide a reasonable approximation over the entire range of possible behavior. Thus the values of N_{oxD} to be developed from Equations 12 and 13 must always be viewed as <u>approximate</u>.

For each available X_1 value, known as a function of the independent variables, Equation 9 can be solved explicitly to obtain the corresponding N_{oxP}; Equation 11 then leads to the <u>exact</u> N_{oxD}.

At given Λ and N_{ox}, two different combinations of P_xB and P_yB can be solved simultaneously (with $\phi = 1$) to obtain values of f_x and f_y. It was noted that, since the definitions of the X and Y phases are arbitrary, f_x and f_y should be closely related. The inversion properties are

$$\Lambda^{\dagger} = 1/\Lambda ,$$

$$N_{ox}^{\dagger} = \Lambda N_{ox} ,$$

and hence

$$f_x (\Lambda, N_{ox}) = f_y (1/\Lambda, \Lambda N_{ox}) . \tag{14}$$

A pair of empirical functions having this property, and fitting the limiting conditions at $N_{ox} = \infty$ and also at $\Lambda = 1$, is

$$f_x = \frac{N_{ox} + \kappa N_{ox}^{2\alpha} \Lambda^{-0.5-\alpha}}{N_{ox} + \kappa N_{ox}^{2\alpha} \Lambda^{-1.5-\alpha}} ,$$

$$f_y = \frac{N_{ox} + \kappa N_{ox}^{2\alpha} \Lambda^{-0.5-\alpha}}{N_{ox} + \kappa N_{ox}^{2\alpha} \Lambda^{+0.5-\alpha}} . \tag{15}$$

A very reasonable fit of these functions to the computed f_x and f_y values is given by the constants $\alpha = 0$, $\kappa = 6.8$. The behavior of f_x and f_y, calculated by use of Equation 15 as a smoothing function, is shown in Figure 14. Other exponents on Λ were investigated, which did not improve the correlation.

Determination of ϕ, as the correction for the difference between correlation values of $(PB)_y$ (from Equation 13) and "exact" N_{oxD}'s, leads to the relation

$$\phi = 1 - \frac{0.050}{\Lambda (PB)_y N_{ox}} . \tag{16}$$

The entire correlation becomes unsatisfactory in the range where ϕ becomes negative.

Typical values of C_{x1} estimated by means of the correlation just presented, using in turn Equations 15, 13, 16, 12/11, and 9, are shown in Table I along with comparative values from the exact computer calculations. The estimated values generally agree within 1% of the feed-concentration level, and therefore appear satisfactory for use in many design calculations. A complete comparison from $\Lambda = 1/16$ to $\Lambda = 1/2$ is given in the Appendix.

Table I

Comparison of approximate and exact raffinate compositions

($\Lambda = 0.25$)

N_{ox}	P_xB	P_yB	X_1	
			Estimated	Computed
2	1.0	0.25	0.3860	0.3844
		1.0	0.3628	0.3728
		4.0	0.3520	0.3518
	4.0	1.0	0.3179	0.3190
		4.0	0.2819	0.2883
		16.0	0.2689	0.2690
8	1.0	0.25	0.2213	0.2178
		1.0	0.1807	0.1906
		4.0	0.1569	0.1468
	4.0	1.0	0.1354	0.1465
		4.0	0.0760	0.0796
		16.0	0.0540	0.0474
	16.0	4.0	0.0396	0.0451
		16.0	0.0156	0.0149
		64.0	0.0105	0.0106

In this correlation, $(PB)_y$ is insensitive to small changes in N_{ox}. Hence it can be evaluated with an inaccurate N_{ox}, and used in Equations 11 and 12 to develop a more accurate value. With the recognition that longitudinal dispersion is often a significant factor in equipment performance, and with the development of calculation methods to account for it, a pressing need has developed for measuring complete concentration profiles in operating equipment -- not merely outlet values -- which will supply more accurate values of transport rates than were heretofore available, along with new quantitative information about dispersion rates.

ACKNOWLEDGMENT

Tables were computed in the University of California Computer Center.

Norman Nian-tze Li assisted in the preparation of the jump-ratio plots.

NOTATION

a	Interfacial area per unit column volume (cm^2/cm^3)
B	L/d (dimensionless)
c_i	Concentration of solute in ith phase ($gm\text{-}moles/cm^3$)
C_i	c_i/c_x^0 (dimensionless), with c_x^0 the feed-stream concentration
d	A length characteristic of the equipment (cm)
D,E,F	Calculation parameters in the evaluation of X at $P_yB = 0$
E_i	Effective longitudinal dispersion coefficient (superficial) in the ith phase (cm^2/sec)
fi	Weighting factor, in Equation 15 (dimensionless)
F_i	Superficial volumetric flow rate of ith phase through unit cross section of the apparatus (cm/sec)
H_{oi}	Height of an over-all transfer unit based on the ith phase (cm)
k_{oi}	Over-all coefficient of mass (or heat) transfer based on the ith phase (cm/sec)
ℓ_i	Mixing length; E_i/F_i (cm)
L	Effective column length in direction of mean flow (cm)
m	Solute partition coefficient; dc_x^*/dc_y (dimensionless)
N_{oi}	Number of over-all transfer units in a column, based on the ith phase; L/H_{oi} (dimensionless)
P_i	Local Péclet number for the ith phase; d/ℓ_i (dimensionless)
Q	Intercept on linear equilibrium plot; $c_x^* = Q + mc_y$ ($gm\text{-}moles/cm^3$)
r_i	Jump ratio in the ith phase; see Equation 6 (dimensionless)
t_i	Temperature in the ith phase (^oC)
X	Generalized solute concentration in the X phase; $[C_x - (Q + m\,C_y^0)]/[1 - (Q + m\,C_y^0)]$ (dimensionless)
Y	Generalized solute concentration in the Y phase; $m(C_y - C_y^0/[1 - (Q + mC_y^0)]$ (dimensionless)

z	Length within the column, measured from the X-phase inlet in the direction of flow (cm)
Z	Fractional length in column; z/L (dimensionless)
α	Adjustable exponent in Equation 15 (dimensionless)
κ	Numerical coefficient in Equation 15 (dimensionless)
Λ	Capacity ratio; mF_x/F_y (dimensionless)
ν	$(1 + 4\ N_{ox}/P_x B)^{1/2}$ (dimensionless)
ϕ	Correlation factor, in Equation 12 (dimensionless)

Subscripts

D	dispersion
i	designates phase concerned, either X or Y
o	Over-all
P	piston-flow model, or exterior apparent value
x,y	designates X or Y phase
0	feed-inlet end, inside column
1	feed-outlet end, inside column

Superscripts

*	equilibrium
†	designates inversion of phase definitions
0	feed-inlet end, outside column
1	feed-outlet end, outside column

LITERATURE CITED

(1) Colburn, A. P., Ind. Eng. Chem. 33, 459 (1941).

(2) Danckwerts, P. V., Chem. Eng. Science, 2, 1 (1953).

(3) Miyauchi, T., UCRL-3911 (August 1957) Longitudinal Dispersion in Two-Phase Continuous Flow Operations; Theoretical Analysis., Ind. Eng. Chem., (paper submitted).

(4) Miyauchi, T., McMullen, A. K., and Vermeulen, T., UCRL-3911-Supplement, (January 1958) Longitudinal Dispersion in Solvent-Extraction Columns; Numerical Tables.

(5) Miyauchi, T., McMullen, A. K., and Vermeulen, T., UCRL-9112, (March 1960), Longitudinal Dispersion in Two-Phase Continuous-Flow Operation; Parallel Flow, Theory and Tables.

(6) Sleicher, C. A., Jr., Am. Inst. Chem. Engrs. J. 5, 145 (1959).

(7) Van Deemter, J. J., Zuiderweg, F. J., and Klinkenberg, A., Chem. Eng. Science, 5, 271 (1956).

(8) Yagi, A., and Miyauchi, T., Kogaku Kikai (Chem. Eng., Japan), 19, 507 (1955).

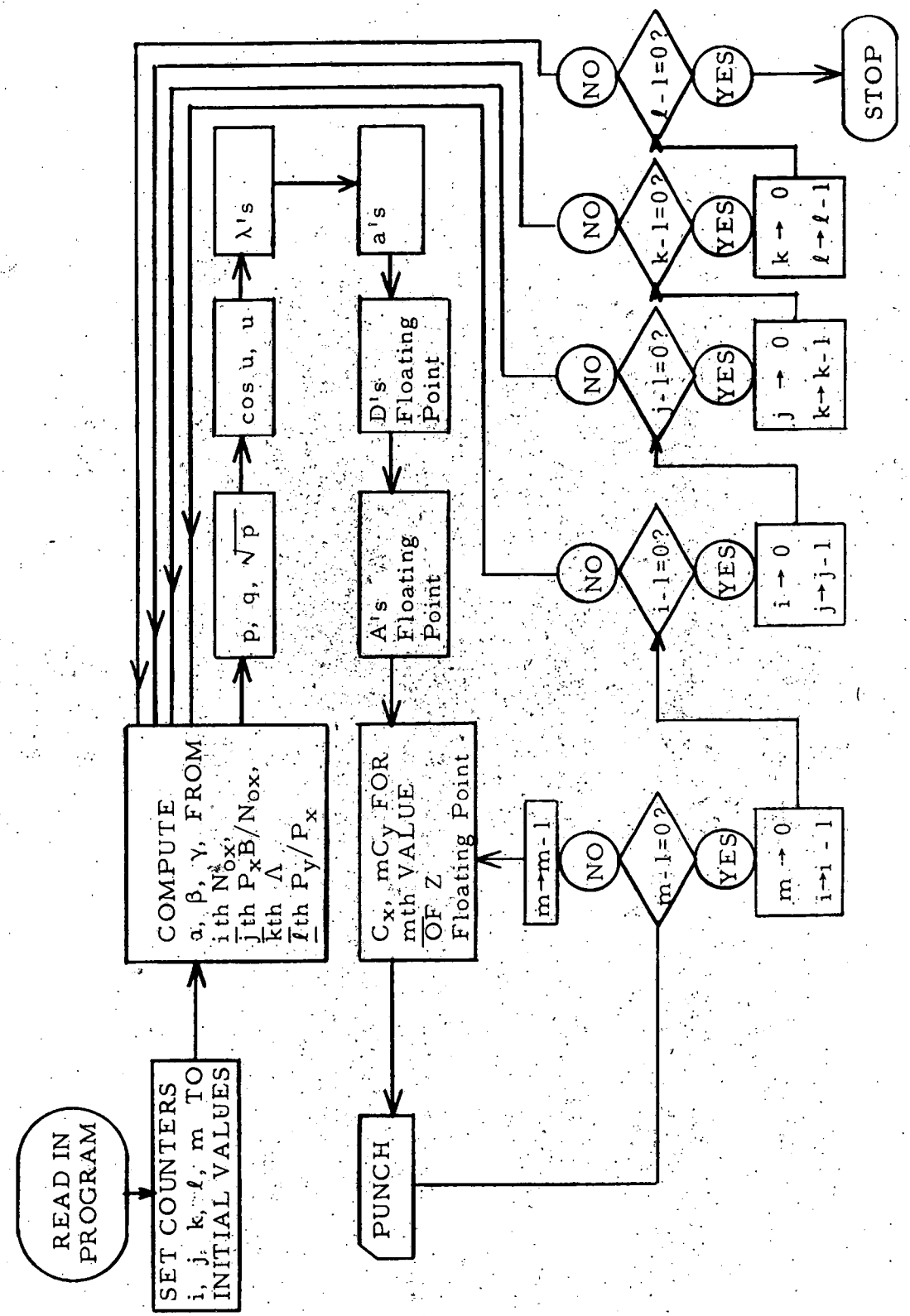

Figure 1. Sequence of operations for evaluation of concentration profiles.

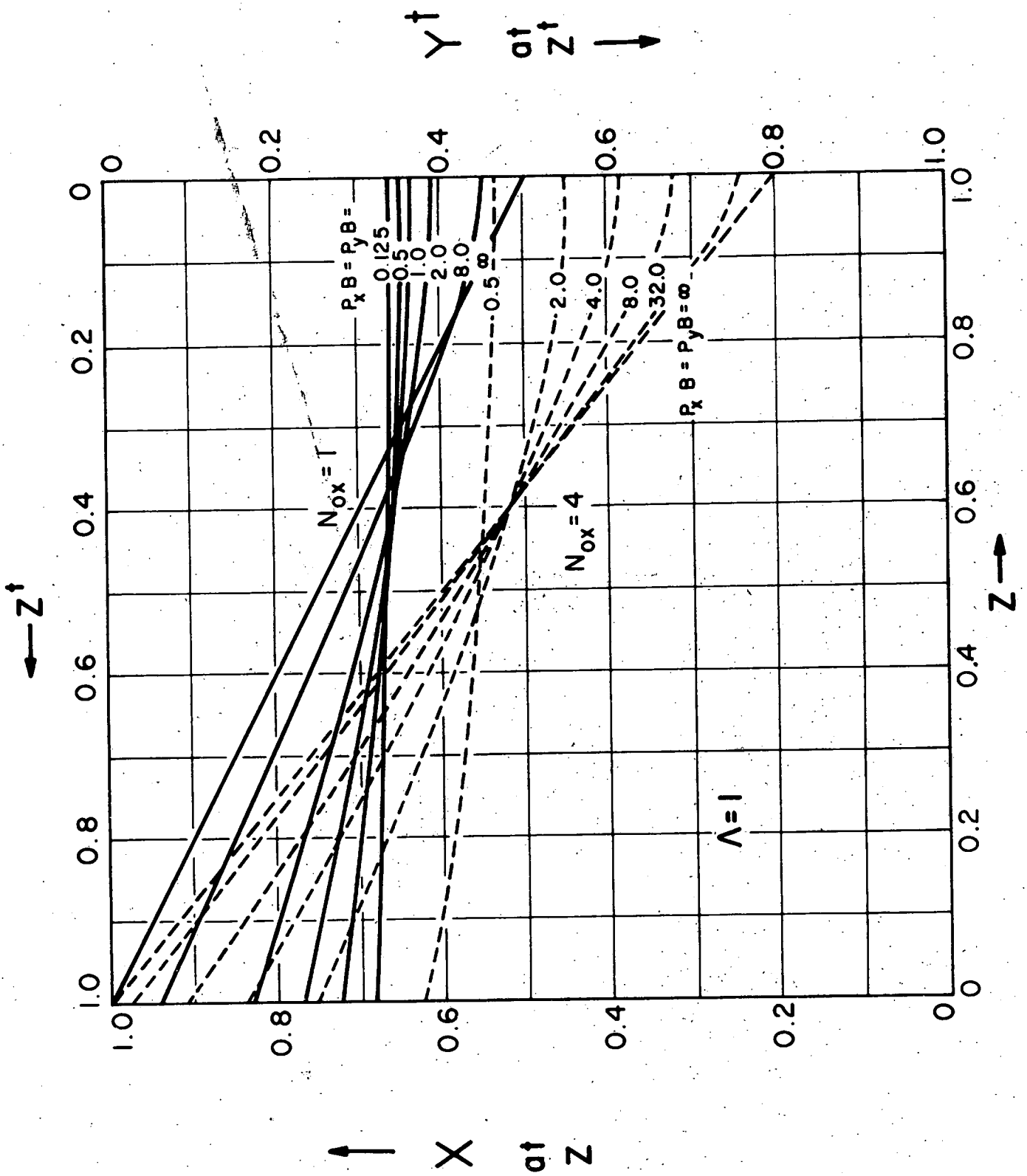

Figure 2. Typical concentration profiles in countercurrent flow, for $\Lambda = 1$.

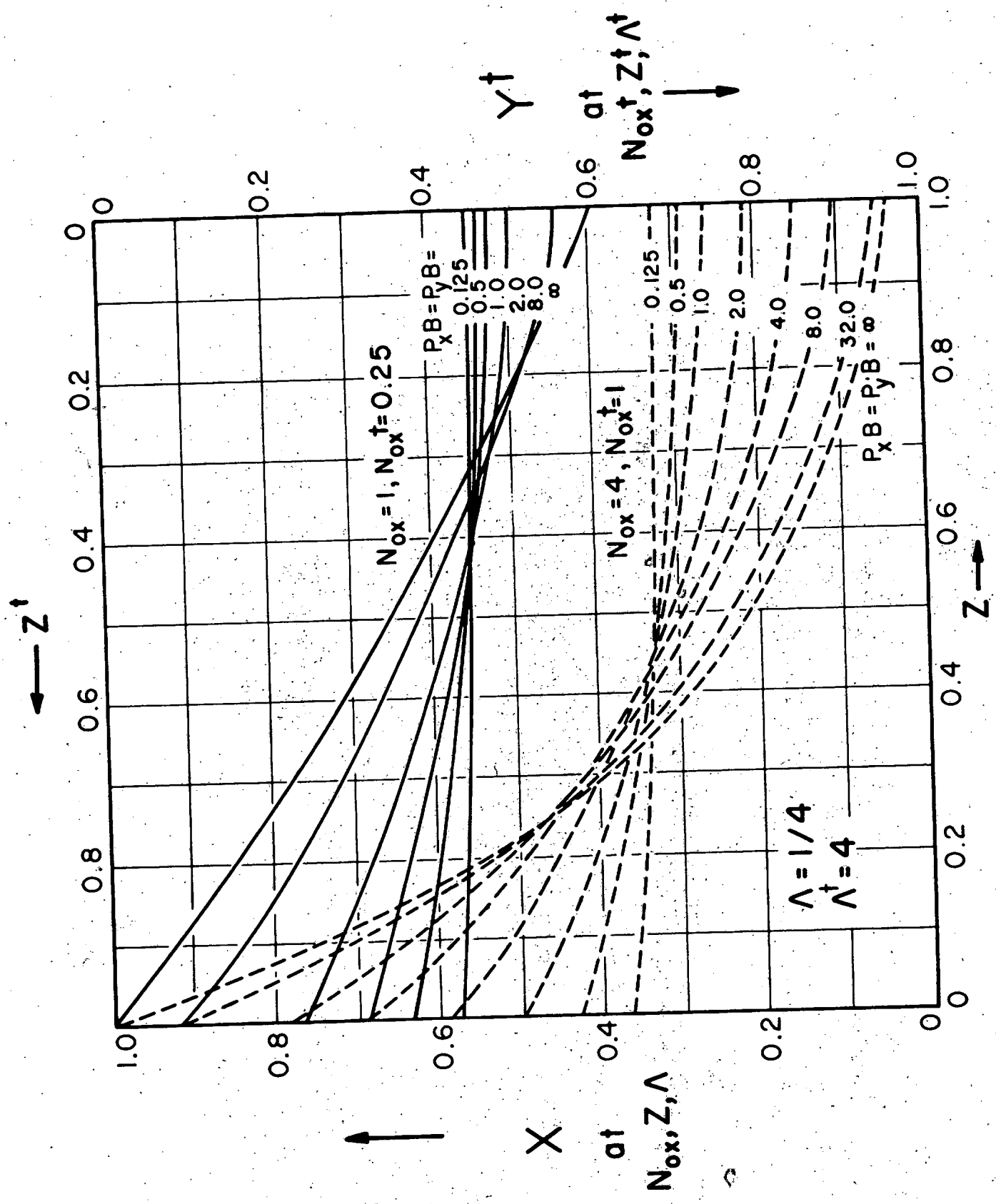

Figure 3. Typical concentration profiles in countercurrent flow, for $\Lambda = 1/4$.

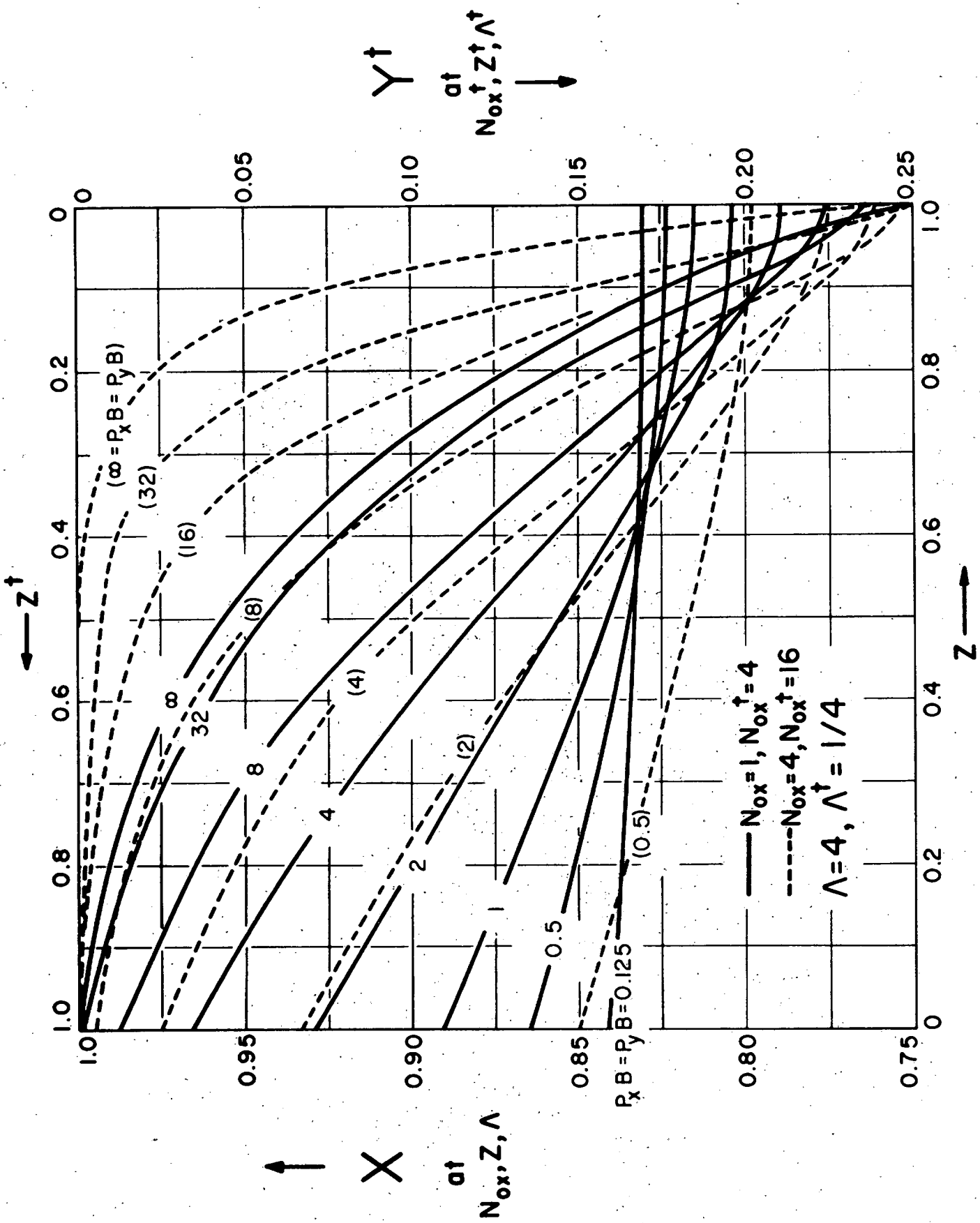

Figure 4. Typical concentration profiles in countercurrent flow, for $\Lambda = 4$.

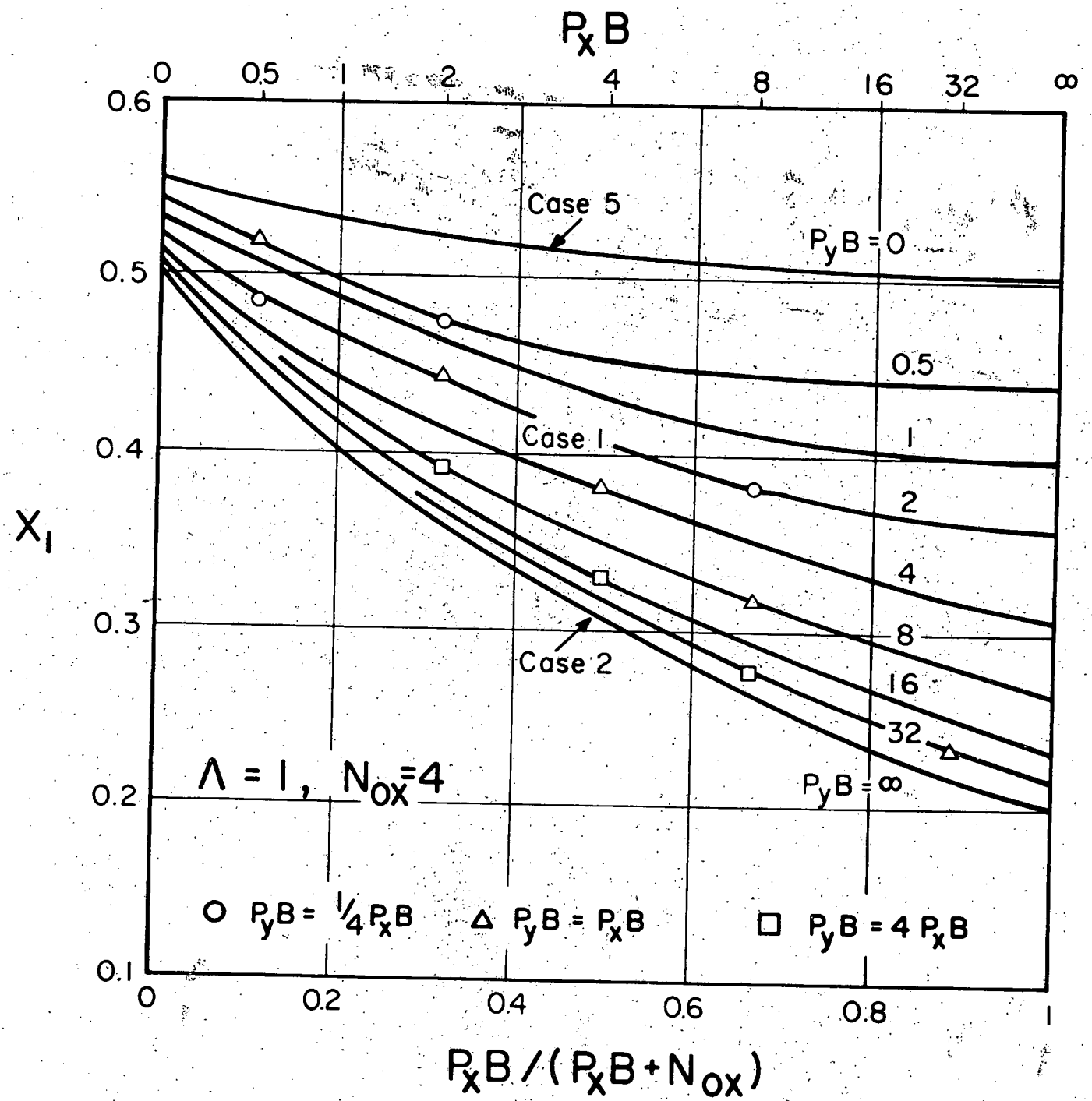

Figure 5. Effect of column Péclet numbers on outlet concentration, at $\Lambda = 1$.

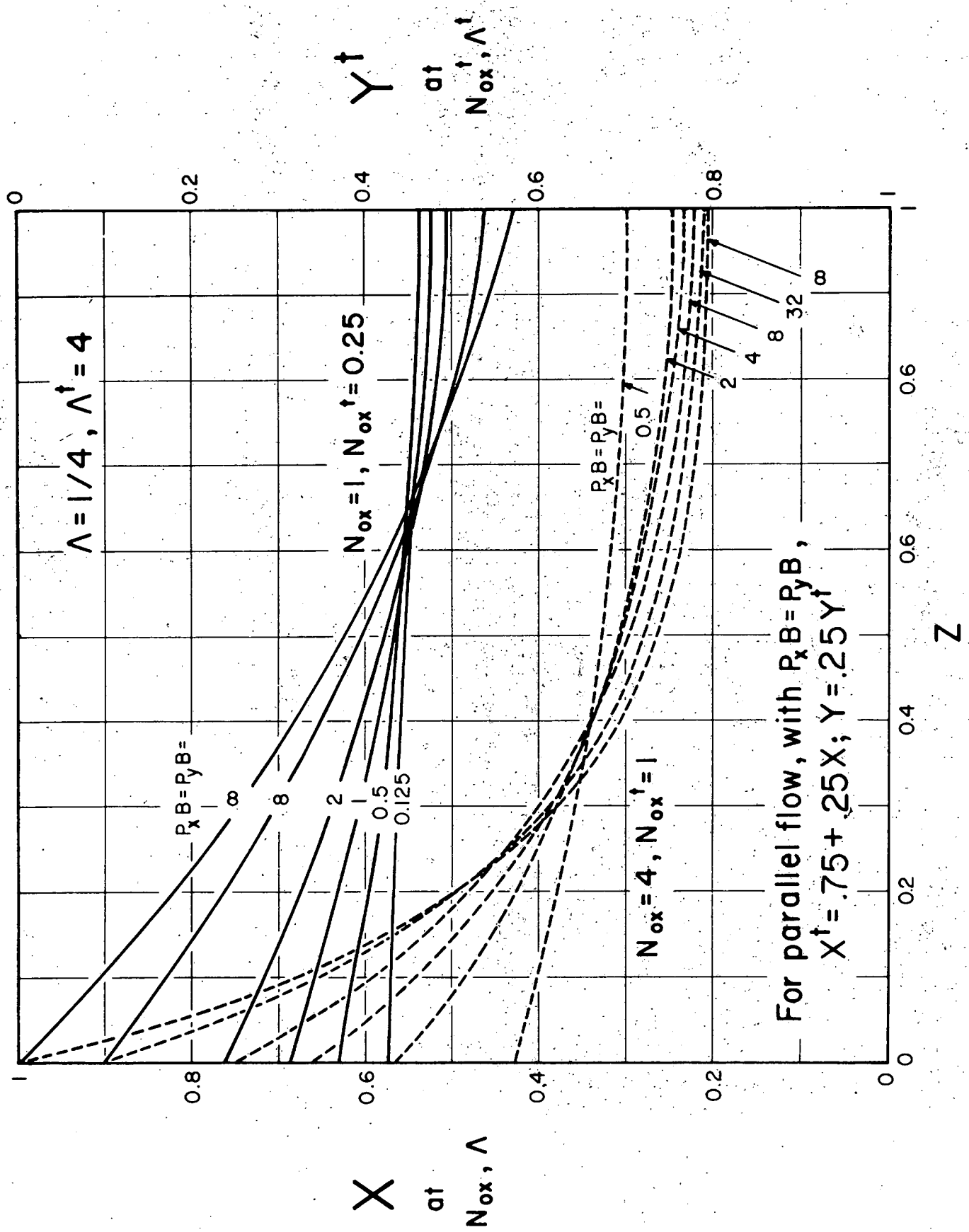

Figure 6. Typical concentration profiles in cocurrent flow, for $\Lambda = 1/4$.

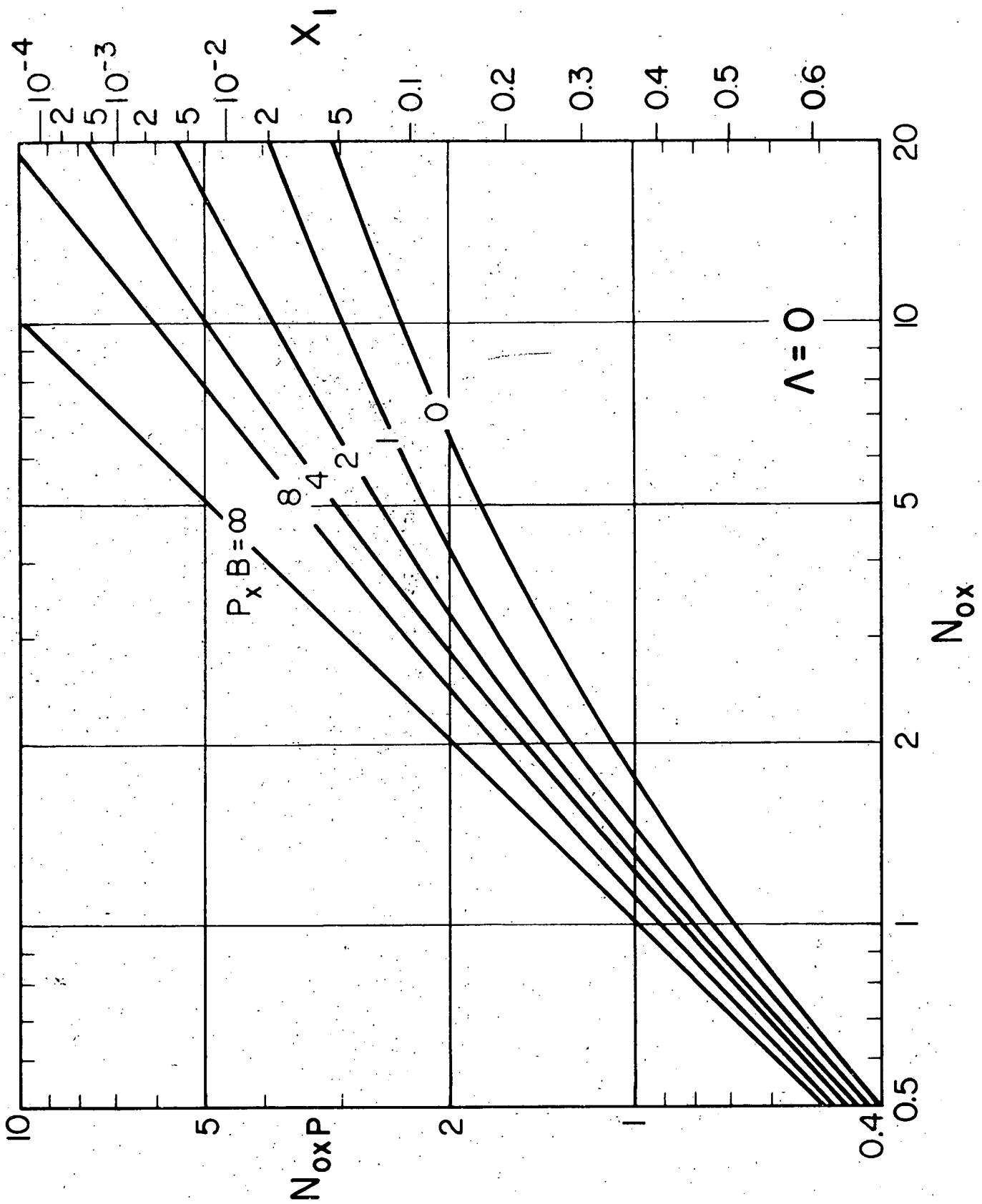

Figure 7. Effect of longitudinal dispersion in the X phase, with constant concentration in the Y phase; outlet concentration X_1.

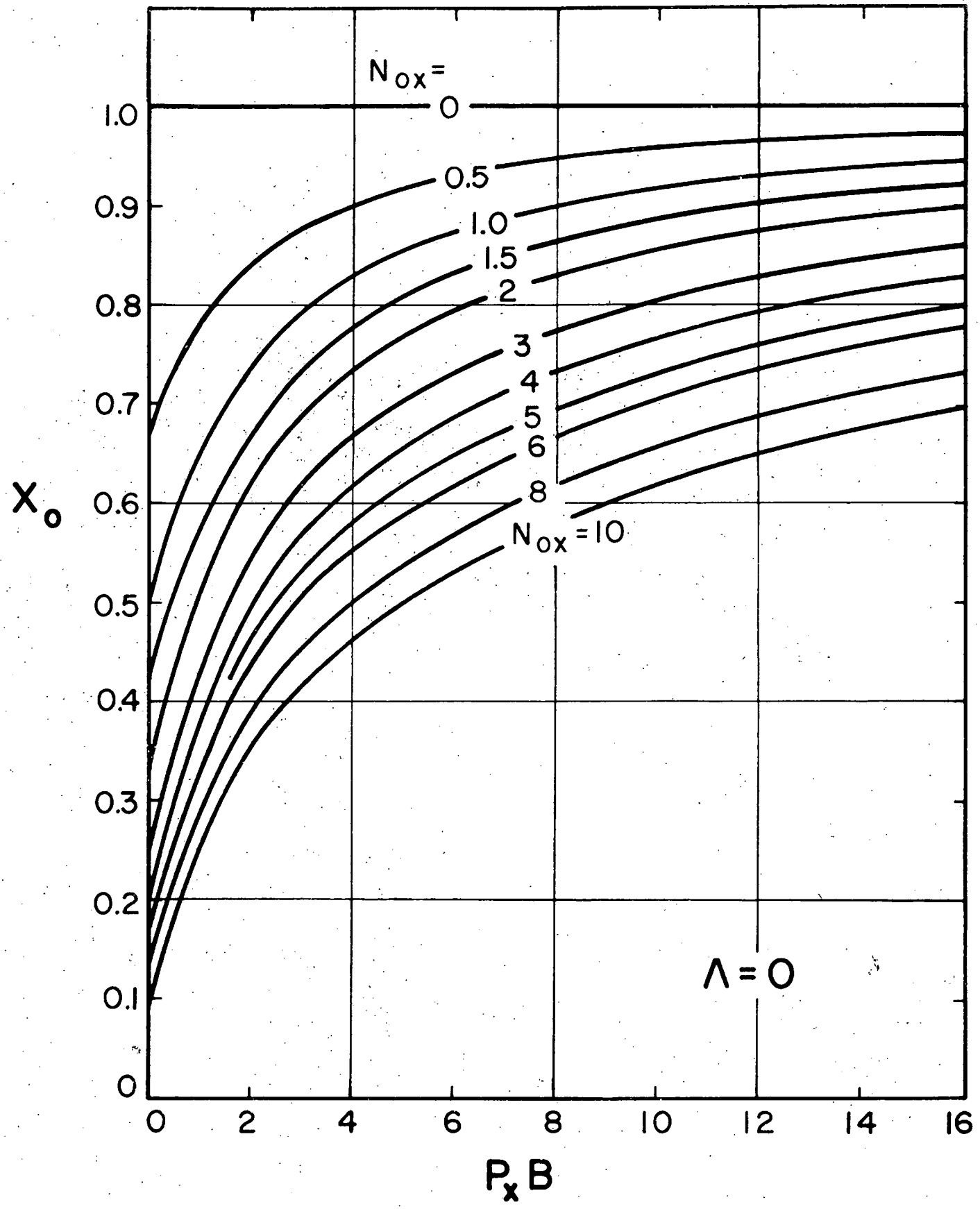

Figure 8. Effect of longitudinal dispersion in the X phase; with constant concentration in the Y phase; inlet-end interior concentration X_o.

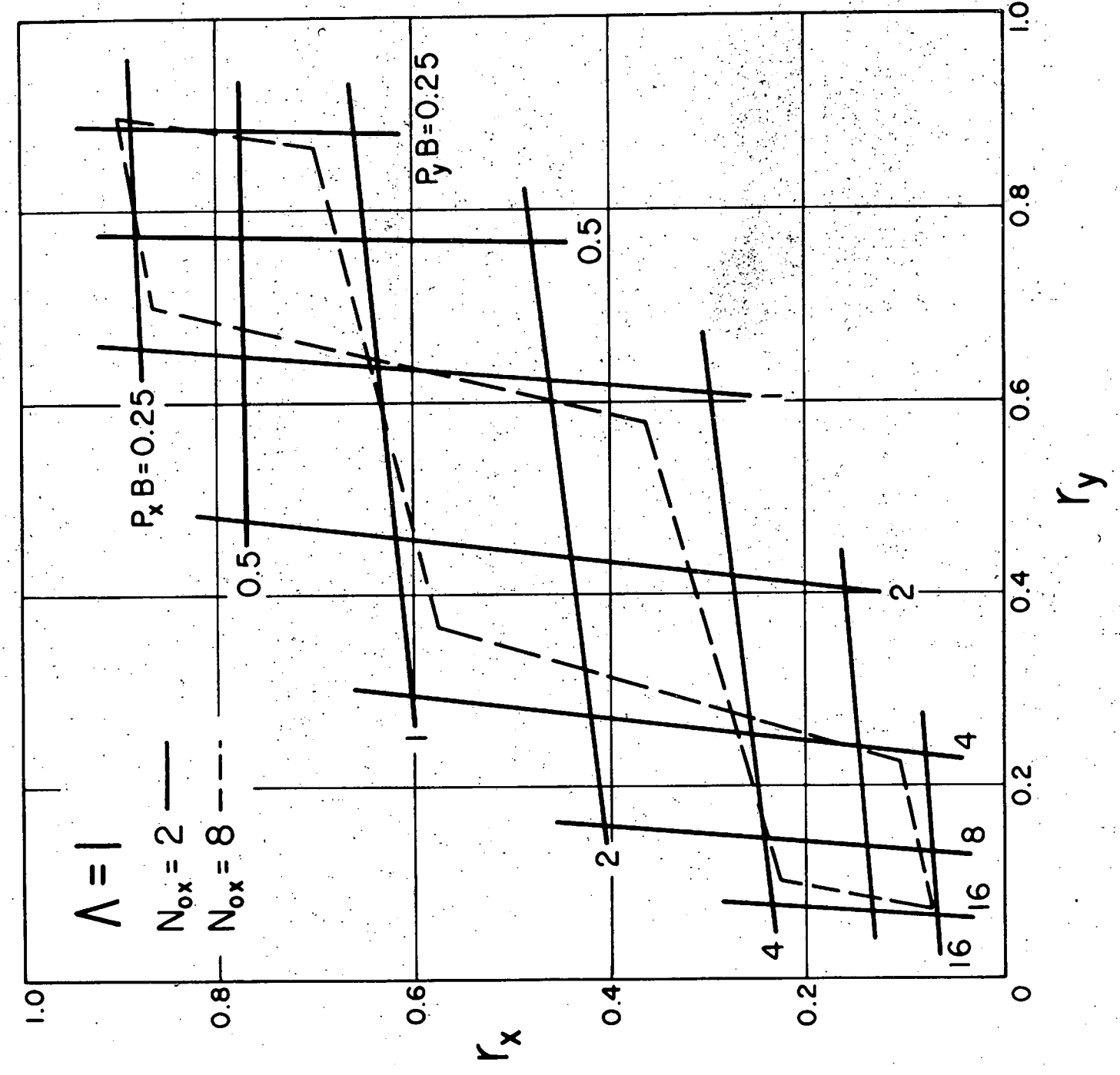

Figure 9. Jump ratios at X-phase and Y-phase inlets, for Λ = 1.

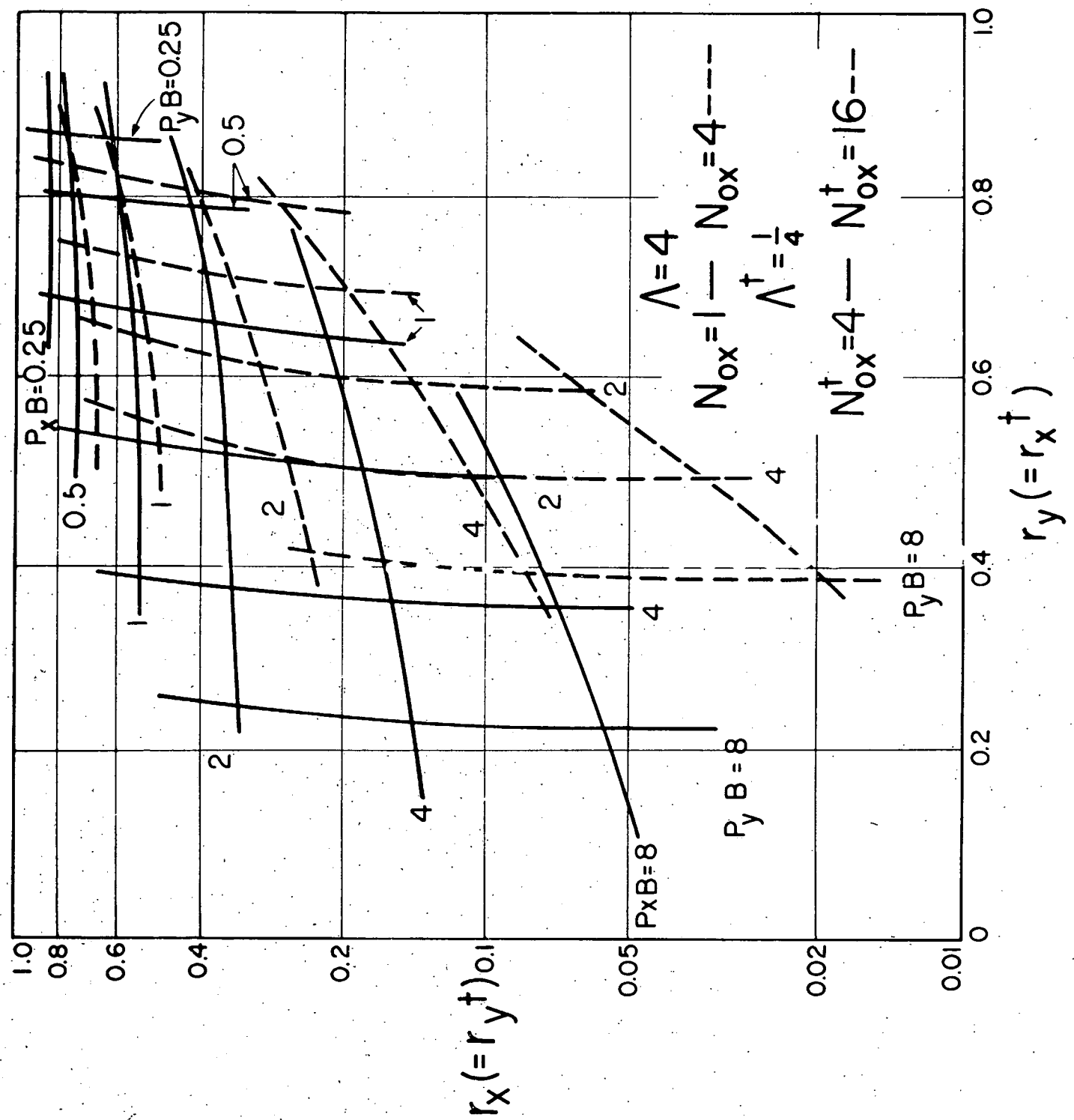

Figure 10, Jump ratios at X-phase and Y-phase inlets, for $\Lambda = 4$.

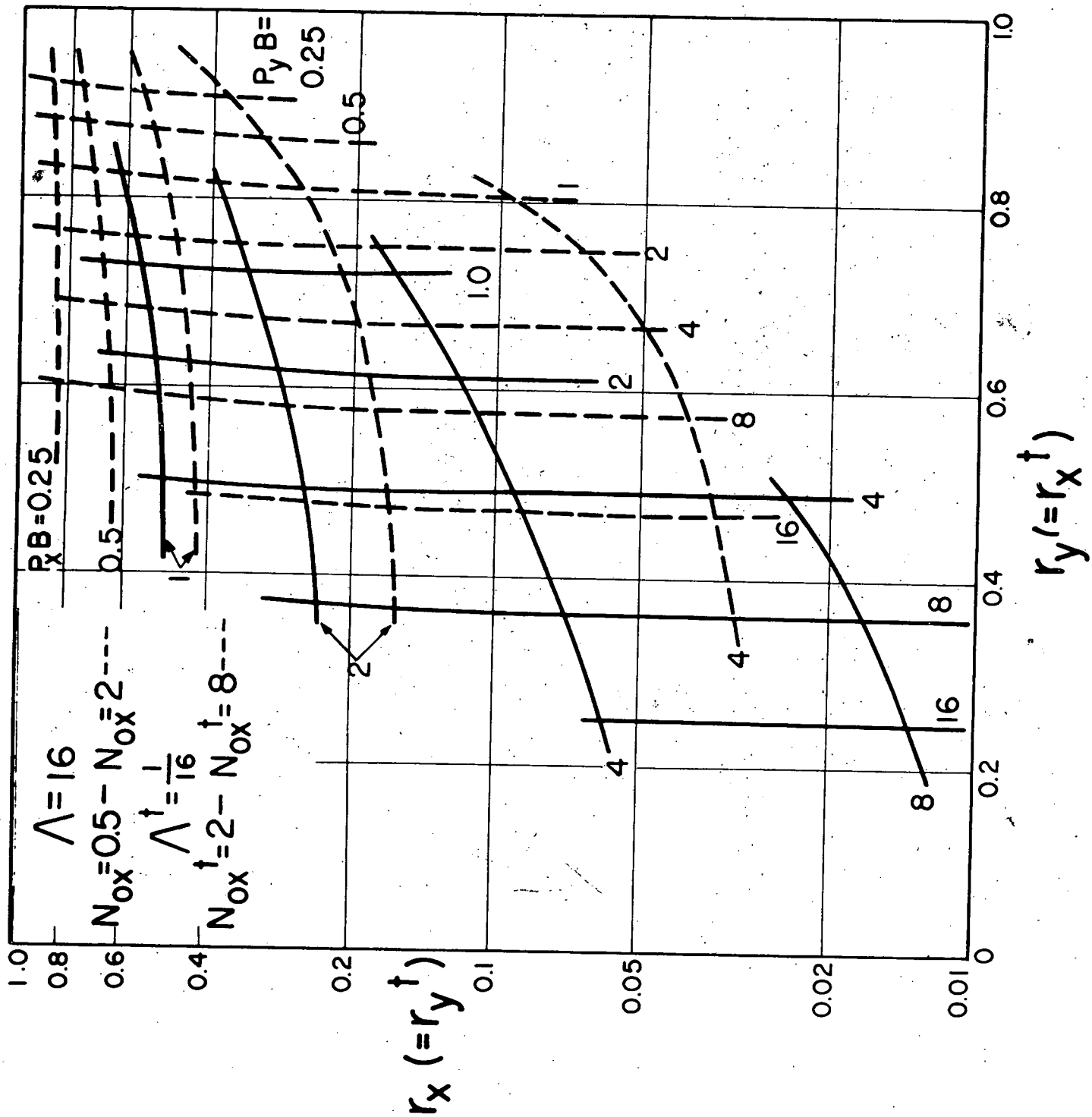

Figure 11. Jump ratios at X-phase and Y-phase inlets, for $\Lambda = 16$.

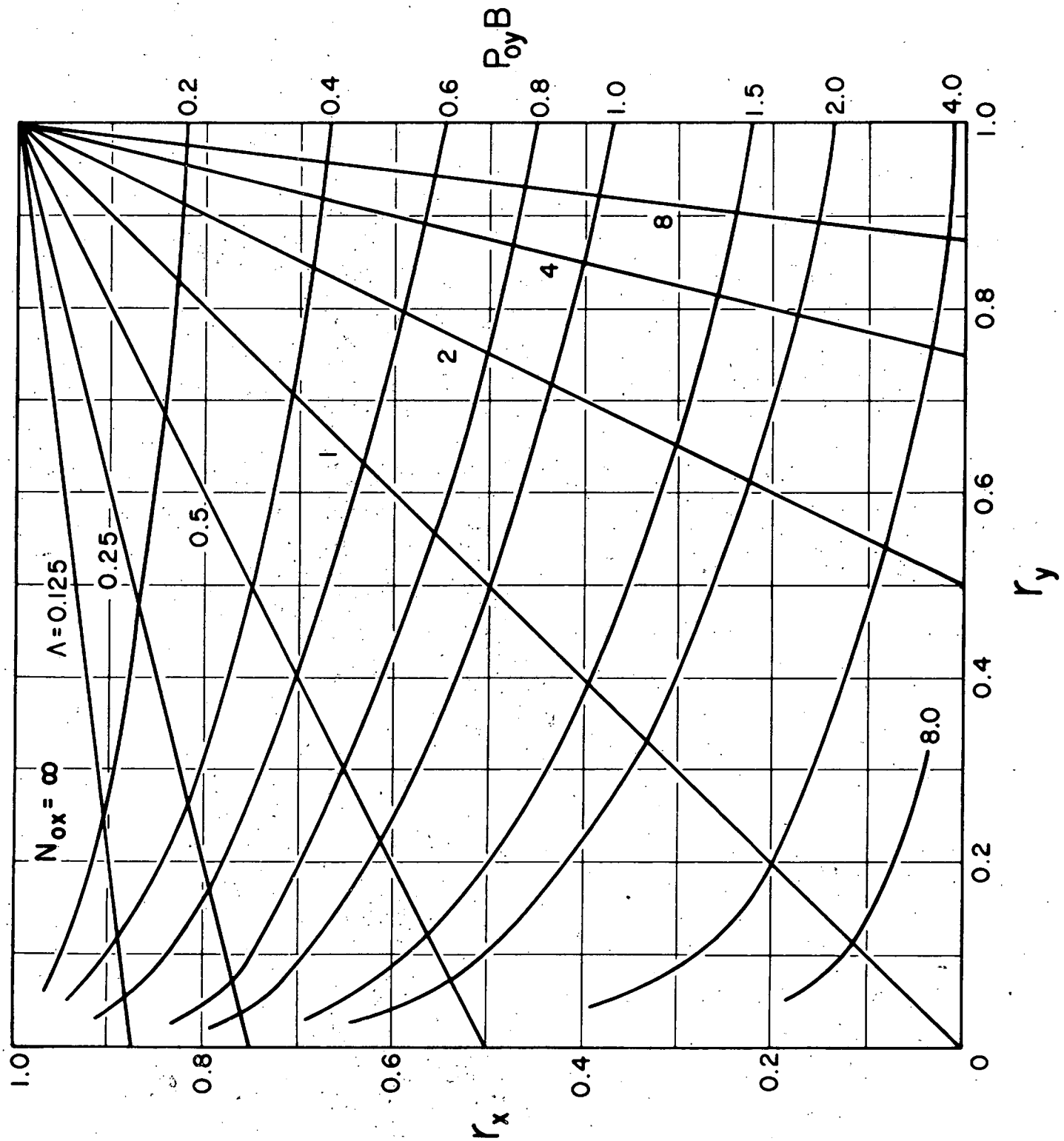

Figure 12. Jump ratios at X-phase and Y-phase inlets, for $N_{ox} = \infty$.

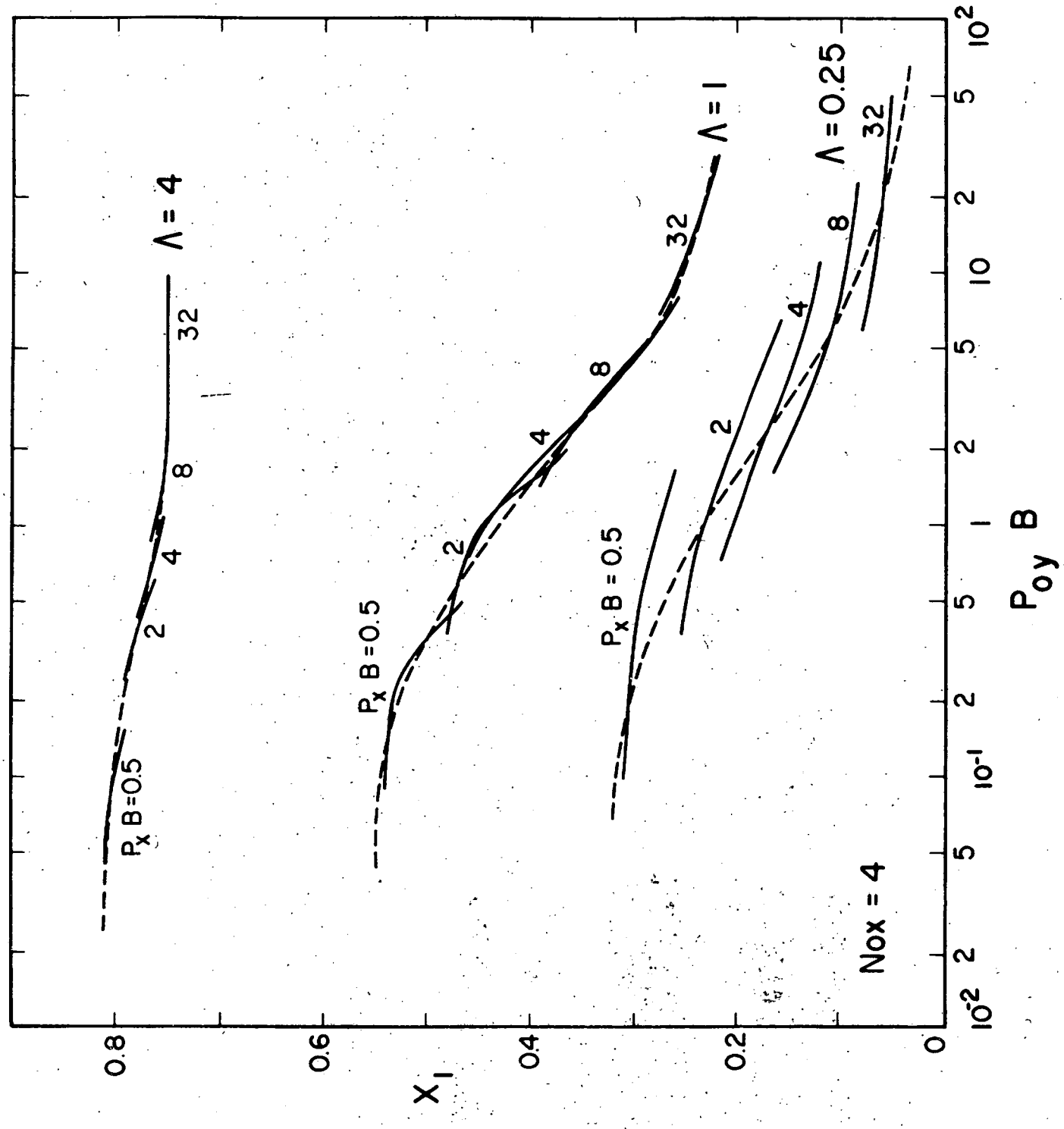

Figure 13. Trial use of $P_{oy}B$ to correlate effect of mixing in both phases.

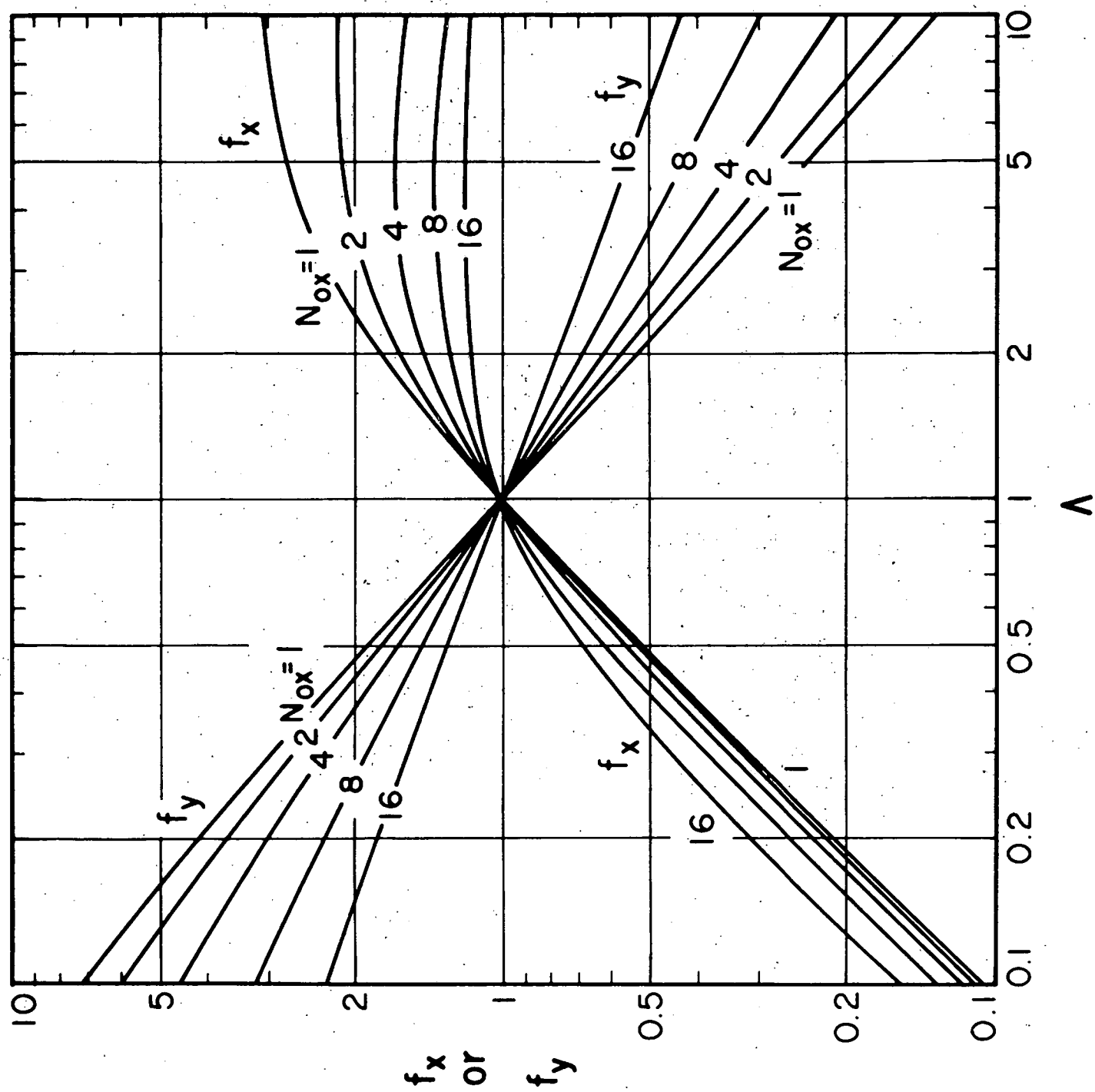

Figure 14. Weighting factors for calculating $(PB)_y$, as functions of Λ and N_{ox}.

LAMBDA	N	OX	PX.B	PY.B	CX1.ESTIM	EXACT
.0625	1		0.125	0.125	.50527	.51009
			0.125	0.50	.50491	.50927
			0.50	0.125	.49442	.49766
			0.50	0.50	.49094	.49673
			0.50	2.00	.48983	.49428
			1.00	0.25	.48153	.48402
			1.00	1.00	.47613	.48220
			1.00	4.00	.47445	.47879
			2.00	0.50	.46267	.46414
			2.00	2.00	.45562	.46095
			2.00	8.00	.45352	.45728
			8.00	2.00	.41788	.41791
			8.00	8.00	.41179	.41329
			8.00	32.00	.41014	.41140
.0625	2		0.25	0.062	.32422	.34407
			0.25	0.25	.32112	.34322
			0.25	1.00	.32005	.34046
			1.00	0.25	.29860	.30883
			1.00	1.00	.28984	.30514
			1.00	4.00	.28694	.29839
			2.00	0.50	.27384	.27856
			2.00	2.00	.26186	.27178
			2.00	8.00	.25810	.26443
			4.00	1.00	.24218	.24346
			4.00	4.00	.22905	.23375
			4.00	16.00	.22518	.22809
			16.00	4.00	.18396	.18304
			16.00	16.00	.17610	.17644
			16.00	64.00	.17401	.17475
.0625	4		0.50	0.125	.18548	.19958
			0.50	0.50	.17772	.19659
			0.50	2.00	.17476	.18902
			2.00	0.50	.14301	.14263
			2.00	2.00	.12618	.13078
			2.00	8.00	.12050	.11906
			4.00	1.00	.11010	.10845
			4.00	4.00	.09228	.09210
			4.00	16.00	.08683	.08412

LAMBDA	N	OX	PX.B	PY.B	CX1.ESTIM	EXACT
.0625	4		8.00	2.00	.07749	.07648
			8.00	8.00	.06326	.06180
			8.00	32.00	.05930	.05806
			32.00	8.00	.03802	.03621
			32.00	32.00	.03318	.03285
.0625	8		1.00	0.25	.09962	.09637
			1.00	1.00	.08428	.08665
			1.00	4.00	.07787	.07080
			4.00	1.00	.05023	.04954
			4.00	4.00	.03145	.02780
			4.00	16.00	.02580	.01975
			8.00	2.00	.02556	.02728
			8.00	8.00	.01356	.01114
			8.00	32.00	.01063	.00870
			16.00	4.00	.01051	.01073
			16.00	16.00	.00525	.00441
			16.00	64.00	.00414	.00383
.125	1		0.125	0.031	.52197	.52474
			0.125	0.125	.52024	.52433
			0.125	0.50	.51957	.52280
			0.50	0.125	.51063	.51261
			0.50	0.50	.50505	.51086
			0.50	2.00	.50297	.50625
			1.00	0.25	.49815	.49940
			1.00	1.00	.48939	.49600
			1.00	4.00	.48627	.48959
			2.00	0.50	.47936	.47991
			2.00	2.00	.46775	.47393
			2.00	8.00	.46390	.46699
			8.00	2.00	.43215	.43234
			8.00	8.00	.42177	.42359
			8.00	32.00	.41881	.41993
.125	2		0.25	0.062	.35914	.36961
			0.25	0.25	.35397	.36803
			0.25	1.00	.35185	.36296
			1.00	0.25	.33183	.33600
			1.00	1.00	.31719	.32921
			1.00	4.00	.31159	.31680

LAMBDA	N OX	PX.B	PY.B	CX1.ESTIM	EXACT
.125	2	2.00	0.50	.30489	.30630
		2.00	2.00	.28483	.29387
		2.00	8.00	.27775	.28019
		4.00	1.00	.26963	.27032
		4.00	4.00	.24755	.25240
		4.00	16.00	.24046	.24166
		16.00	4.00	.20221	.20192
		16.00	16.00	.18887	.18927
		16.00	64.00	.18521	.18590
.125	4	0.50	0.125	.23172	.23668
		0.50	0.50	.21877	.23129
		0.50	2.00	.21290	.21778
		2.00	0.50	.18193	.18021
		2.00	2.00	.15356	.15886
		2.00	8.00	.14276	.13725
		4.00	1.00	.14185	.14241
		4.00	4.00	.11149	.11253
		4.00	16.00	.10140	.09713
		8.00	2.00	.10058	.10274
		8.00	8.00	.07600	.07505
		8.00	32.00	.06885	.06742
		32.00	8.00	.04825	.04653
		32.00	32.00	.03976	.03945
.125	8	1.00	0.25	.14572	.14080
		1.00	1.00	.11961	.12359
		1.00	4.00	.10686	.09558
		4.00	1.00	.07929	.08356
		4.00	4.00	.04536	.04365
		4.00	16.00	.03436	.02730
		8.00	2.00	.04276	.04916
		8.00	8.00	.01985	.01777
		8.00	32.00	.01417	.01217
.250	1	0.125	0.031	.55361	.55128
		0.125	0.125	.55089	.55052
		0.125	0.50	.54954	.54776
		0.50	0.125	.54257	.54002
		0.50	0.50	.53370	.53690
		0.50	2.00	.52956	.52873

LAMBDA	N	OX	PX.B	PY.B	CX1.ESTIM	EXACT
.250	1		1.00	0.25	.53014	.52760
			1.00	1.00	.51610	.52157
			1.00	4.00	.51002	.51018
			2.00	0.50	.51085	.50885
			2.00	2.00	.49199	.49827
			2.00	8.00	.48464	.48582
			8.00	2.00	.45906	.45940
			8.00	8.00	.44153	.44367
			8.00	32.00	.43614	.43685
.250	2		0.25	0.062	.41429	.41518
			0.25	0.25	.40620	.41245
			0.25	1.00	.40198	.40386
			1.00	0.25	.38596	.38440
			1.00	1.00	.36278	.37289
			1.00	4.00	.35200	.35186
			2.00	0.50	.35712	.35593
			2.00	2.00	.32500	.33488
			2.00	8.00	.31166	.31121
			4.00	1.00	.31789	.31900
			4.00	4.00	.28192	.28838
			4.00	16.00	.26889	.26906
			16.00	4.00	.23758	.23883
			16.00	16.00	.21498	.21577
			16.00	64.00	.20850	.20921
.250	4		0.50	0.125	.30319	.30145
			0.50	0.50	.28323	.29260
			0.50	2.00	.27201	.27090
			2.00	0.50	.24703	.24653
			2.00	2.00	.20177	.21161
			2.00	8.00	.18153	.17508
			4.00	1.00	.19896	.20399
			4.00	4.00	.14871	.15401
			4.00	16.00	.12990	.12582
			8.00	2.00	.14598	.15333
			8.00	8.00	.10330	.10447
			8.00	32.00	.08991	.08902
			32.00	8.00	.07170	.07083
			32.00	32.00	.05573	.05560

LAMBDA	N	OX	PX.B	PY.B	CX1.ESTIM	EXACT
.250	1		1.00	0.25	.53014	.52760
			1.00	1.00	.51610	.52157
			1.00	4.00	.51002	.51018
			2.00	0.50	.51085	.50885
			2.00	2.00	.49199	.49827
			2.00	8.00	.48464	.48582
			8.00	2.00	.45906	.45940
			8.00	8.00	.44153	.44367
			8.00	32.00	.43614	.43685
.250	2		0.25	0.062	.41429	.41518
			0.25	0.25	.40620	.41245
			0.25	1.00	.40198	.40386
			1.00	0.25	.38596	.38440
			1.00	1.00	.36278	.37289
			1.00	4.00	.35200	.35186
			2.00	0.50	.35712	.35593
			2.00	2.00	.32500	.33488
			2.00	8.00	.31166	.31121
			4.00	1.00	.31789	.31900
			4.00	4.00	.28192	.28838
			4.00	16.00	.26889	.26906
			16.00	4.00	.23758	.23883
			16.00	16.00	.21498	.21577
			16.00	64.00	.20850	.20921
.250	4		0.50	0.125	.30319	.30145
			0.50	0.50	.28323	.29260
			0.50	2.00	.27201	.27090
			2.00	0.50	.24703	.24653
			2.00	2.00	.20177	.21161
			2.00	8.00	.18153	.17508
			4.00	1.00	.19896	.20399
			4.00	4.00	.14871	.15401
			4.00	16.00	.12990	.12582
			8.00	2.00	.14598	.15333
			8.00	8.00	.10330	.10447
			8.00	32.00	.08991	.08902
			32.00	8.00	.07170	.07083
			32.00	32.00	.05573	.05560

LAMBDA	N	OX	PX.B	PY.B	CX1.ESTIM	EXACT
.250	8		1.00	0.25	.22129	.21786
			1.00	1.00	.18071	.19060
			1.00	4.00	.15688	.14688
			4.00	1.00	.13544	.14652
			4.00	4.00	.07600	.07968
			4.00	16.00	.05403	.04745
			8.00	2.00	.08131	.09419
			8.00	8.00	.03626	.03605
			8.00	32.00	.02401	.02239
			16.00	4.00	.03955	.04517
			16.00	16.00	.01559	.01497
			16.00	64.00	.01047	.01064
			64.00	16.00	.00777	.00680
			64.00	64.00	.00408	.00402
.250	16		2.00	0.50	.15683	.16340
			2.00	2.00	.09267	.10125
			2.00	8.00	.05901	.04784
			8.00	2.00	.05607	.07062
			8.00	8.00	.01276	.01256
			8.00	32.00	.00453	.00373
			16.00	4.00	.01910	.02513
			16.00	16.00	.00243	.00211
			16.00	64.00	.00073	.00075
			32.00	8.00	.00408	.00446
			32.00	32.00	.00038	.00032
			28.00	32.00	.00011	.00006
.250	32		4.00	1.00	.09871	.11214
			4.00	4.00	.02886	.03207
			4.00	16.00	.00775	.00536
			16.00	4.00	.01314	.01795
			16.00	16.00	.00040	.00032
			16.00	64.00	.00002	.00002
			32.00	8.00	.00152	.00190
			32.00	32.00	.00001	
			64.00	64.00		

LAMBDA	N OX	PX.B	PY.B	CX1.ESTIM	EXACT
.250	64	8.00	2.00	.04598	.05473
		8.00	8.00	.00313	.00336
		8.00	32.00	.00009	.00006
		32.00	8.00	.00093	.00119
		32.00	32.00		
		64.00	16.00	.00001	.00001
		64.00	64.00		
.500	1	0.125	0.031	.60252	.59629
		0.125	0.125	.59874	.59507
		0.125	0.50	.59617	.59064
		0.50	0.125	.59239	.58650
		0.50	0.50	.57988	.58151
		0.50	2.00	.57216	.56852
		1.00	0.25	.58066	.57544
		1.00	1.00	.56059	.56584
		1.00	4.00	.54942	.54770
		2.00	0.50	.56177	.55810
		2.00	2.00	.53418	.54133
		2.00	8.00	.52094	.52117
		8.00	2.00	.50632	.50716
		8.00	8.00	.47892	.48167
		8.00	32.00	.46955	.46989
.500	2	0.25	0.062	.49353	.48902
		0.25	0.25	.48271	.48490
		0.25	1.00	.47522	.47222
		1.00	0.25	.46677	.46278
		1.00	1.00	.43503	.44582
		1.00	4.00	.41625	.41514
		2.00	0.50	.43839	.43680
		2.00	2.00	.39330	.40597
		2.00	8.00	.37033	.37044
		4.00	1.00	.39767	.40007
		4.00	4.00	.34529	.35482
		4.00	16.00	.32305	.32402
		16.00	4.00	.30523	.30847
		16.00	16.00	.26932	.27089
		16.00	64.00	.25828	.25898
.500	4	0.50	0.125	.40649	.40284
		0.50	0.50	.38071	.39042
		0.50	2.00	.36238	.36160

LAMBDA	N	OX	PX.B	PY.B	CX1.ESTIM	EXACT
.500	4		2.00	0.50	.34990	.35216
			2.00	2.00	.28789	.30428
			2.00	8.00	.25417	.25274
			4.00	1.00	.29772	.30638
			4.00	4.00	.22444	.23623
			4.00	16.00	.19199	.19140
			8.00	2.00	.23478	.24586
			8.00	8.00	.16682	.17207
			8.00	32.00	.14245	.14321
			32.00	8.00	.13097	.13209
			32.00	32.00	.10048	.10088
.500	8		1.00	0.25	.33696	.33724
			1.00	1.00	.28499	.30168
			1.00	4.00	.24844	.24789
			4.00	1.00	.23975	.25451
			4.00	4.00	.15024	.16230
			4.00	16.00	.10962	.10762
			8.00	2.00	.16847	.18476
			8.00	8.00	.08775	.09251
			8.00	32.00	.06022	.06035